Effect of cold Ar plasma treatment on the catalytic performance of Pt/CeO$_2$ in water-gas shift reaction (WGS)

Laura Pastor-Pérez[a], Victor Belda-Alcázar[a], Carlo Marini[b], M. Mercedes Pastor-Blas[a], Antonio Sepúlveda-Escribano[a], Enrique V. Ramos-Fernandez[a,*]

[a] *Laboratorio de Materiales Avanzados, Departamento de Química Inorgánica, Instituto Universitario de Materiales de Alicante, Universidad de Alicante, Apartado 99, E-03080 Alicante, Spain*
[b] *ALBA Synchrotron, Cerdanyola del Vallès, 08290 Barcelona, Spain*

ARTICLE INFO

ABSTRACT

The effect of Ar plasma treatment on the catalytic performance of Pt/CeO$_2$ has been studied. The catalyst was activated using different procedures separately or in combination: calcination, reduction under pure H$_2$ and cold Ar plasma treatment. The resulting materials were characterized by X-ray photoelectron spectroscopy, X-ray adsorption near edge structure and temperature-programmed reduction with H$_2$. The resulting materials were tested in the water-gas shift reaction (WGS). It has been found that the combination of calcination, plasma and hydrogen treatments leads to a very active catalyst for WGS. Furthermore, the catalyst structure–performance relationship has been assessed. The plasma treatment generated electron-enriched Pt particles which show a very strong interaction with the ceria support. This favoured CO chemisorption and increased the reducibility of the support, which takes part in the WGS the reaction by favouring water splitting.

1. Introduction

The water-gas shift reaction (WGS) is a key step in the purification of gas streams coming from steam reformer units. Actually, this reaction is the first stage of the purification process. Industrially, WGS is carried out in two consecutive steps, at high and low temperatures, respectively. It requires large facilities since a cooler is needed between the two differently heated units.

In order to build miniaturized portable fuel processor systems, it is necessary to develop advanced medium-temperature shift (MTS) catalysts suitable for a single-stage WGS reaction. MTS-catalysts are generally based on noble metals supported on reducible oxides. These metals are highly active phases and the oxide support has also an important role as a redox buffer. In this sense, Pt/CeO$_2$ is a promising catalyst for the water-gas shift reaction (WGS) [1–9].

Supported metal catalysts are traditionally prepared by impregnating a support material with the metal precursor solution, followed by calcination at a relatively elevated temperature and/or reduction under hydrogen (generally above 300 °C). The resulting metal particles are usually heterogeneously dispersed, with a broad particle size distribution [10,11]. The impregnation procedure determines how the precursor metal species spread and anchor on the support. When these impregnated supports are submitted to calcination and/or reduction,

the resulting dispersion of the Pt particles is not only dependent on the treatment itself but also on the type of species formed upon impregnation. The interaction between the noble metal and the support is crucial to promote a synergetic cooperation between the redox properties of the support and the activity of the noble metal [12,13].

Traditionally, this interaction is induced by the pre-treatments to which the catalyst is submitted for activation. Thus, calcination at relatively high temperatures (above 300 °C) causes the decomposition of the metal precursor and, in some cases, the reaction of the generated compounds with the support. This is the case, for example, of the formation of nickel aluminates upon calcination of an alumina support impregnated with nickel nitrate. During calcination of ceria-supported platinum precursors, the generated Pt-O-Ce species favor a good metal dispersion and an appropriate metal-support interaction in the final catalyst. On the other hand, reduction under hydrogen not only produces metal particles but also favours surface reduction of partially reducible supports such as ceria by a spillover mechanism. The generated redox pairs might also participate in the catalytic process [14–17].

Recently, the use of plasma treatments for the synthesis and activation of catalysts has attracted considerable attention. Plasma treatment is a simple, easy to manipulate green technique, which may become an environmentally friendly alternative to conventional catalysts synthesis, usually involving the use of hazardous solvents and

---

* Corresponding author.
E-mail addresses: enrique.ramos@ua.es, e.v.ramosfernandez@me.com (E.V. Ramos-Fernandez).

chemicals. There is a wide variety of plasmas and their classification can be made on the basis of the power supply used to generate them, the pressure of the working gas, the geometry of the electrode and the nature of the discharge. Thus, low-pressure and atmospheric pressure plasmas are available. On the other hand, depending on their energy level, temperature and electronic density, plasma is classified as high temperature (thermal) plasma and cold (non-thermal or non-equilibrium) plasma. Non-thermal plasmas have been considered very promising due their non-equilibrium properties, low power requirement and their capacity to induce physical and chemical reactions within gases at relatively low temperatures. The electrons in non-thermal plasma can reach temperatures of 10,000–100,000 K (1–10 eV) while the gas temperature can remain as low as room temperature. There is a wide variety of non-thermal plasmas, including low-pressure plasmas and high (atmospheric pressure) plasmas. The corona discharge is an inhomogeneous discharge initiated at atmospheric pressure. The main drawback of the atmospheric plasma systems is their limited working space due to the small gap between the electrodes. On the other hand, low pressure-non thermal plasmas include glow discharge, dielectric barrier discharge (DBD), gliding arc discharge, radio frequency (RF) and microwave (MW) plasmas. The RF discharge operates at high frequencies (e.g. 13.56 MHz) and very low pressure to achieve the non-equilibrium conditions, while the MW discharge operates at very high frequencies (e.g. 2.45 GHz) in the range of microwaves.

A non-thermal plasma is a mixture of electrons, highly excited atoms and molecules, ions, radicals, fotons, etc. The chemistry involving plasma reactions is therefore quite complex. Several plasma-assisted catalytic reactions have been reported, however not many studies try to explain the observed boosted catalytic activity. In this context, the aim of this work is to study the effects of a cold Ar RF plasma treatment on the catalytic performance of a Pt/CeO_2 catalyst in the water-gas shift reaction (WGS). The WGS reaction is highly interesting due to its sensitivity to metal dispersion, metal-support interaction and redox properties of the catalyst. Furthermore, the Pt/CeO_2 system has largely demonstrated high performance in WGS reaction [4].

2. Experimental

2.1. Catalysts preparation

CeO_2 was prepared by precipitation from an aqueous solution of Ce $(NO_3)_3 \cdot 6H_2O$ (99.99%, Sigma-Aldrich) containing an excess of urea. The solution was heated at 80 °C and kept at this temperature, with slow stirring for 12 h. The solid formed was filtered and calcined at 350 °C for 4 h. After synthesis of the support, the Pt/CeO_2 catalyst was prepared by impregnation with an excess of solvent. The corresponding amount of $H_2PtCl_6 \cdot 6H_2O$ (99.99%, Alfa Aesar) was dissolved in acetone to obtain 1 wt.% Pt. Calcined CeO_2 was added to the solution, in a proportion of 10 mL$g_{support}$$^{-1}$, with stirring. After 12 h, the excess of solvent was slowly removed under vacuum and the solid was then dried in an oven until complete removal of the solvent. Finally, part of the solid was calcined for 4 h at 350 °C. In this way, two ceria-supported samples were prepared and labelled as Pt/CeO_2-f (fresh) and Pt/CeO_2-c (calcined). Prior to reaction, samples were reduced at 350 °C for 2 h under flowing hydrogen (50 mL min^{-1}), and they were labelled as Pt/CeO_2-f H_2 and Pt/CeO_2-c H_2.

2.2. Plasma treatment

The Pt/CeO_2 catalysts (both fresh and calcined) were loaded on an aluminium boat, which was placed in the glow discharge stainless steel cylindrical chamber of a Tucano plasma system (Gambetti Kenologia, Italy), provided with an anodized aluminium door. The HF electrode is made of aluminium and has a "Dark Shield", an RF 13.56 MHz power supply and mass flow controllers (MFC) for gas inlet control. The reaction chamber was evacuated under mild vacuum (0.15 Torr) using a

Pfeiffer rotary vane pump (model PK D41 029C-Duo 2.5 with F4 Fomblin lubricant YL VAC 25/6). Ar (99.9999% minimum purity, Air Liquid) was introduced into the plasma chamber over the specimen. Care was taken to pump down and purge the plasma reactor for at least 10 min prior to activating the RF field. The discharge power was set to 200 W. Plasma treatment was performed in 20 cycles of 5 min each, with manual mixing of the sample between cycles to assure an even exposure to the plasma. The temperature of the sample after the plasma treatment was measured by a non-contact infrared thermometer (PCE Instruments, model PCE-888). The surface temperature was below 80 °C in all cases. The samples treated with plasma were labelled Pt/CeO_2-f Plasma and Pt/CeO_2-c Plasma. Finally, a part of these samples was submitted to a conventional reduction treatment (50 mL min^{-1} H_2, 2 h at 350 °C). Therefore, samples treated with plasma and plasma + H_2 were labelled as Pt/CeO_2-f Plasma, Pt/CeO_2-f Plasma + H_2, Pt/CeO_2-c Plasma and Pt/CeO_2-c Plasma + H_2.

2.3. Catalysis characterisation

Temperature-programmed reduction (TPR) with H_2 experiments were carried out on the fresh, calcined and treated with plasma catalysts in a U-shaped quartz cell using a 5% H_2/He gas flow of 50 mL min^{-1}, with a heating rate of 10 °C min^{-1}. Hydrogen consumption was followed by on-line mass spectrometry.

X-Ray photoelectron spectroscopy was performed with a K-ALPHA spectrometer (Thermo Scientific). All spectra were collected using Al-$K\alpha$ radiation (1486.6 eV), monochromatized by a twin crystal monochromator, yielding a focused X-ray spot with a diameter of 400_m, at 3 mA × 12 kV. The alpha hemispherical analyser was operated at the constant energy mode with survey scan pass energies of 200 eV to measure the whole energy band and 50 eV in a narrow scan to selectively measure the particular elements. Charge compensation was achieved with the system flood gun that provides low energy electrons and low energy argon ions from a single source. The C 1 s core level was used as reference binding energy, and it is located at 284.6 eV. The powder samples were pressed and mounted on the sample holder and placed in the vacuum chamber. Before recording the spectrum, the samples were maintained in the analysis chamber until a residual pressure of ca. 5 × 10^{-7} N m^{-2} was reached. The quantitative analysis was estimated by calculating the integral of each peak, after subtracting the S-shaped background, and by fitting the experimental curve to a combination of Lorentzian (30%) and Gaussian (70%) lines. Plasma treated and reduced samples were conserved in octane solution (inert atmosphere). Suspensions were evaporated in the XPS chamber under vacuum conditions.

2.4. X-Ray absorption near edge structure

XANES spectra were collected at CLÆS, the X-ray absorption dedicated beamline of the national Spanish synchrotron source (ALBA). The calcined catalyst and the plasma treated one were submitted to a hydrogen reduction treatment at different temperatures, making use of the multipurpose solid gas reactor available in the beamline setup pool. Due to total absorption problem, measurements at Pt L_3 edge were performed in fluorescence mode while spectra at Ce L_3 edge were collected in transmission mode. Detectors (used in these experiments) were standard ionization chambers (filled with an adequate mixture of gases to assure a correct statistics counting of incoming and outcoming photon beams) and a silicon drift fluorescence detector from Amptek.

2.5. Catalytic behaviour

The catalytic behaviour of the prepared samples in the water-gas shift reaction was evaluated in a fixed bed flow reactor under atmospheric pressure in the range of temperatures from 160 to 360 °C. Experiments were carried out with a feed gas composition of 5% CO

and 30% H_2O in helium (total flow of 100 mL min^{-1}). Activity tests were performed using 0.150 g of catalyst diluted in SiC, to avoid thermal effects. The corresponding contact time was 0.09 g s mL^{-1} and the Gas Hour Space Velocity (GHSV) was 40000 mL g^{-1} h^{-1}. The composition of the gas stream exiting the reactor was analysed by mass spectrometry (Pfeiffer, OmniStar GSD 301), and the catalytic activity was expressed by the degree of CO conversion as a function of the reaction temperature. The stabilization time for each temperature was 1 h and the CO conversion percentage was calculated by this equation:

CO conversion (%) = 100–(x CO/x CO$_{initial}$)·100

where x CO is the concentration of CO in the outlet of the reactor and x CO$_{initial}$ is the CO concentration in the initial gas mixture. The carbon balance was checked taking into account all the carbon-containing products. The error in CO conversion for all the experiments is within ± 0.5%

3. Results and discussion

The prepared catalysts were characterized by several techniques in order to understand the effect of plasma treatment on their surface properties, and how these changes on surface properties can affect the redox properties and the catalytic behaviour of the materials. Thus, X-ray photon-electron spectroscopy (XPS) was combined with X-ray absorption near edge structure (XANES).

Discussion of XPS results will be focused on the Pt 4f core level rather than in other elements, even though other elements, such as Cl, O, or C were also detected in all samples. Cl 2$p_{3/2}$ at 198.2 eV was assigned to Cl anions present as impurities coming from the Pt precursor (hexachoroplatinic acid). Carbon moieties from surface contamination were also been detected (C1 s was always centred at 284.6 eV). Fig. 1 shows the Pt 4f core level for the calcined and fresh samples after several treatments.

The XPS spectrum of the calcined sample (Pt/CeO$_2$–c) (Fig. 1a) can be deconvoluted into four peaks, two of them (located at 72.9 and 74.3 eV) correspond to the 4$f_{7/2}$ core level and the other two peaks (at 75.8 and 77.6 eV) correspond to the 4$f_{5/2}$ level (Table 1). The fact that both levels can be deconvoluted into two peaks reveals that two different platinum species are formed after calcination. They are electron deficient-species and are ascribed to oxidic platinum (Pt^{n+}) present in two different oxidation states, Pt^{2+} (72.9 eV) and Pt^{4+} (74.8 eV). This suggests that during the calcination of the catalyst, partial reduction of Pt species takes place. This fact has been thoroughly reported in the literature [14,19,20]. Considering that XPS is a surface-sensitive technique, the oxidation state of platinum in the bulk has been determined by XANES. Fig. 2 shows the Pt L$_3$ transition for calcined samples after several treatments. A clearly pronounced main absorption peak (white line) at Pt L$_3$ edge, reaching a maximum of 2.35 in the normalized spectrum μ(E) is observed. As already reported in the literature, the absorption edge is located around 11564 eV. This occurs when oxidic platinum is present, which is in agreement with the XPS results and confirms that bulk and the surface Pt-species have the same nature [21].

When the calcined sample is summited to a reduction treatment under hydrogen at 350 °C Pt/CeO$_2$-c H$_2$), the XPS spectrum shows only one kind of Pt species [22–25] with contributions at 72.0 eV (4$f_{7/2}$) and 75.3 eV (4$f_{5/2}$) (Table 1), which can be ascribed to Pt in an considerable lower oxidation state, nearly close to that of the metal (Pt^0). However, these binding energies are slightly higher than those reported for unsupported Pt^0 (4$f_{7/2}$ at 71.8 eV), usually consisting of larger platinum particles. This is probably due to the lack of relaxation that Pt atoms experience after the photoemission event, what commonly happens when Pt is highly dispersed. It could also be due to the partial reduction of the support. Pt/Ce atomic ratios calculated by XPS are 0.0168 for the calcined sample (Pt/CeO$_2$-c) and 0.0145 for the calcined and reduced
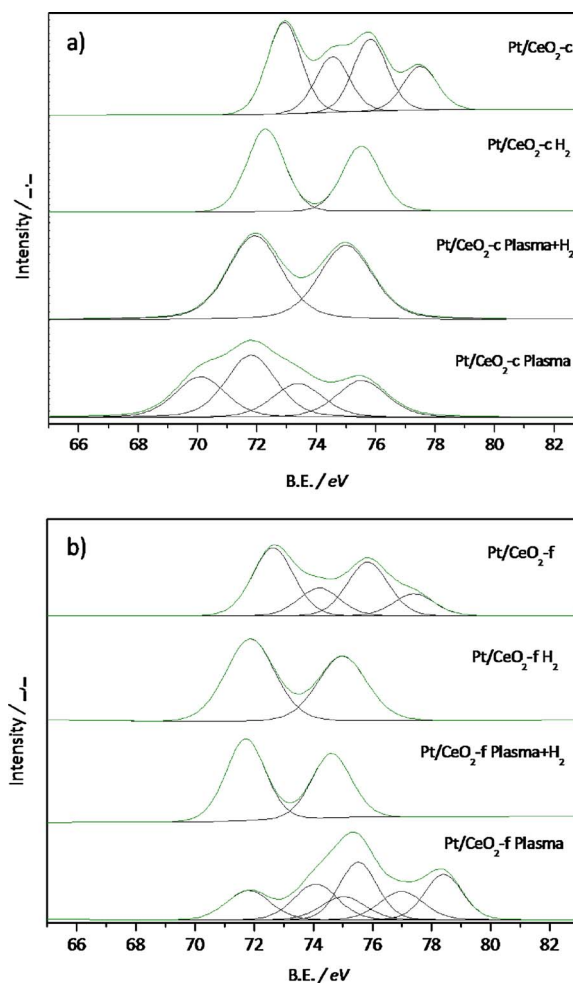

Fig. 1. Pt 4f core level for a) calcined and b) fresh samples.

Table 1
Binding energies of the Pt 4f level for the different samples, as well as the Pt/Ce atomic ratio calculated with XPS.

	Pt 4$f_{7/2}$	Pt 4$f_{5/2}$	Pt/Ce atomic ratio	Ce^{3+} (%)
Calcined samples				
Pt/CeO$_2$-c	72.9–74.3	75.8–77.6	0.0168	32.2
Pt/CeO$_2$-c H$_2$	72.0	75.3	0.0145	35.1
Pt/CeO$_2$-c Plasma + H$_2$	71.8	75.0	0.0119	40.3
Pt/CeO$_2$-c Plasma	69.9–71.9	73.3–75.3	0.0395	39.9
Fresh samples				
Pt/CeO$_2$-f	72.6–74.4	75.9–77.4	0.0413	37.4
Pt/CeO$_2$-f H$_2$	71.7	74.9	0.0079	36.9
Pt/CeO$_2$-f Plasma + H$_2$	71.8	75.0	0.0029	34.5
Pt/CeO$_2$-f Plasma	71.9–74.8-75.5	73.1–77.1-78.5	0.1090	39.6

sample (Pt/CeO$_2$-c H$_2$). Those values are above the nominal loading (0.0089), as expected (Table 1). Considering the crystal structure of ceria it is possible to make an estimation of the maximum surface area covered by a 2D layer of ceria (521.6 m^2/g). Comparing this value with that provided by B.E.T. (110 m^2/g) the percentage of ceria at the surface can be calculated. Thus, the maximum theoretical surface Pt/Ce atomic ratio is 0.041. Pt/Ce atomic ratios obtained from XPS quantification are therefore lower than the theoretical estimation. This can be explained in terms of Pt sintering to form Pt particles which interact with ceria. XPS is therefore able to detect a few layers of ceria below the outermost surface. The estimated surface relative amount of Ce^{3+} is
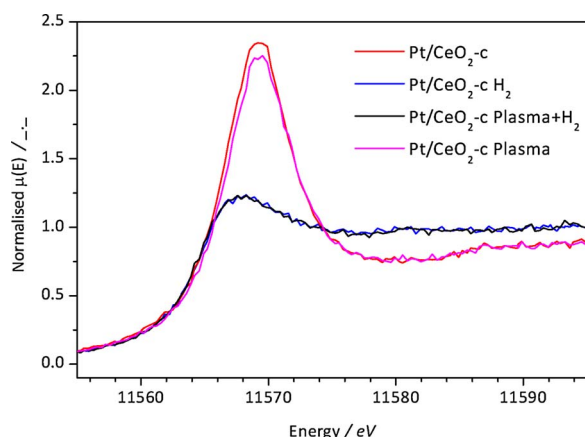
Fig. 2. Pt L_3 transition for calcined samples after several treatments.

~35%. These findings suggest that calcination and calcination plus reduction treatments enhance the interaction between ceria and platinum, as expected.

The corresponding XANES spectrum (Fig. 2) of shows a decrease of the normalized energy of the L_3 transition (1.3) in comparison with the spectrum of the calcined sample not submitted to the hydrogen reduction treatment (2.4). These findings evidence the presence of metallic platinum. Therefore, the combination of XPS and XANES allows confirming that the reduction treatment is effective in producing metal Pt nanoparticles.

On the other hand, when the sample is calcined and then treated with Ar plasma (Pt/CeO$_2$-c Plasma) two different Pt species are present. XPS spectrum (Fig. 1) shows two $4f_{7/2}$ contributions at 69.9 and 71.9 eV (Table 1). The binding energy at 71.9 eV may be ascribed to Pt^0, however, the peak at 69.9 eV is located at an unusual low binding energy, which suggests that the Pt atoms have a high electron density. After checking the largest existing XPS database, that of the National Institute of Standards and Technology (NIST) [26] it can be affirmed that this low binding energy has been never reported for Pt, which suggests that the plasma treatment produces a new type of Pt species. As the XPS device is provided with a flood gun to counteract the charging of the non-conducting samples as ceria, this unusual low binding energy may be due to the nature of the sample itself and not to the charging of the sample during the XPS experiment. Besides, the fact that the Ce 3d core level is not shifted, as expected in the case that the sample was charged, confirms the presence of Pt species with an unusually low binding energy.

XANES spectroscopy is useful to determine the nature of Pt species by comparison of data with the Pt L_3 edge XANES data of Pt foil, PtO$_2$ and K$_2$PtCl$_4$ reference materials: Pt foil ($\mu(E) = 1.3$), PtO$_2$ ($\mu(E) = 3.2$) and K$_2$PtCl$_4$ ($\mu(E) = 1.7$). White lines of Pt/CeO$_2$-c and Pt/CeO$_2$-c Plasma samples reach a maximum of 2.35 and 2.25 respectively, which suggests the presence of multiple Pt species.

Taking into account the XPS and XANES data for these samples, and considering that XPS is a surface sensitive technique and XANES is bulk sensitive, these findings suggest the presence of core-shell Pt particles with a shell composed of reduced platinum and a core made of oxidic platinum [27]. The reducing ability of Ar plasma is due to the presence of highly energetic electrons [18,28]. The stability of the platinum species formed upon air exposure is enhanced by the presence of platinum and cerium in different oxidation states (Pt^{n+}/Pt^0) and (Ce^{4+}/Ce^{3+}). These redox pairs help to stabilize charges at the surface. The core-shell structure might be responsible for the unusual low binding energy found at the Pt 4f level of the plasma-treated samples.

The Pt/Ce ratio of the plasma treated sample (Pt/CeO$_2$-c Plasma) (0.0395) is very close to the theoretical one (0.041) and almost three times higher than those of the samples not treated with plasma (Table 1). It might indicate that plasma is producing a re-dispersion of

platinum or cleaning the catalyst surface more efficiently than the other treatments. Besides, Ce^{3+} content is 39.9%, indicating that plasma not only affects the platinum species but also the surface ceria. The high percentage of Ce^{3+} at the surface as well as the low measured Pt binding energy indicate that plasma produces Pt particles with high electron density, which are stabilized by electron donation from ceria enhanced by its n-type semiconductor behaviour.

Therefore, the combination of calcination and plasma treatments induced a strong Pt-ceria interaction which results in an the modification of the Pt electron density. This is possible because the Ce 4f level, which lies ~2 eV below the Fermi level, is partially occupied when ceria is reduced and the Pt° ($6s^2 + 5d^8$) band has a high electron density at the Fermi level [25]. Consequently, it is possible the electron transfer between the partially reduced ceria and Pt in close contact.

When the calcined sample is treated with plasma and further submitted to a hydrogen treatment (Pt/CeO$_2$-c Plasma + H$_2$) single Pt species are detected by XPS, with binding energies (B.E.) centred at 71.8 eV ($4f_{7/2}$) and 75.0 eV ($4f_{5/2}$) (Table 1). These B.E. values are ascribed to reduced Pt (similar species were detected by XANES) however, they are 0.2 eV lower than those obtained for the sample that had been reduced but not treated with plasma (Pt/CeO$_2$-c H$_2$). This is consequent with a plasma activation of the sample surface that enhances further reduction by H$_2$ treatment. However, the reduced Pt species detected in the plasma-treated sample (Pt/CeO$_2$-c Plasma) (69.9 eV) do not show up when this sample is further submitted to a H$_2$ treatment at 350 °C (Pt/CeO$_2$-c Plasma + H$_2$). In order to find an explanation for that, it is interesting to study if plasma and hydrogen treatments affect the ceria support., so XPS analysis of the Ce 3d core level and XANES analysis at the Ce L_3 edge have been carried out (Supporting information-S.I.).

XPS spectra of the Ce 3d core level of samples calcined and then treated with plasma (Pt/CeO$_2$-c Plasma), calcined and treated with hydrogen (Pt/CeO$_2$-c +H$_2$), and calcined and treated with plasma and hydrogen (Pt/CeO$_2$-c Plasma + H$_2$) are quite similar in terms of binding energies. However, the percentage of Ce^{3+} is very high (40.3%) for the calcined and plasma-treated sample (Pt/CeO$_2$-c Plasma), but much lower for the calcined and hydrogen-treated sample (sample Pt/CeO$_2$-c + H$_2$). This suggests that plasma treatment enhances Pt-ceria interaction, which it is also reflected after hydrogen treatment [16].

XANES measurements might throw some light on the matter. XANES spectra of samples treated with H$_2$ show a shift of the edge of Ce L_3 to lower energy, which suggests a partially reduction of Ce^{4+} to Ce^{3+} [29,30]. Consequently, the n-type semiconductor character of the ceria support and its electron density would be increased. This might affect the electron density on the Pt nanoparticles, which is considerably less important in the H$_2$ treated samples as confirmed by XPS measurements, where no contribution of Pt $4f_{7/2}$ at 69.9 eV is detected.

Summarizing, it can be stated that the plasma treatment mainly affects surface platinum species, as assessed by XPS and XANES studies.

Similar analyses were conducted for the un-calcined (fresh) Pt/CeO$_2$ catalysts. The Pt 4f core spectrum (Fig. 1b) of the Pt/CeO$_2$-f shows four peaks, which are ascribed to two different platinum species (Table 1). The one at higher binding energies (74.4 eV for Pt $4f_{7/2}$) may be ascribed to Pt coordinated to chloride anions from the Pt precursor (PtCl$_x$) [14].

When the fresh sample is reduced with H$_2$ at 350 °C (Pt/CeO$_2$-f H$_2$) there is a shift of the Pt 4f spectrum to lower binding energies (71.7 and 74.9 eV, Table 1), indicating that the Pt precursor is reduced to Pt^0, as expected. Pt 4f spectrum of the fresh sample treated with plasma (Pt/CeO$_2$-f Plasma), widens and new contributions show up (Table 1), which may be ascribed to oxidic platinum with high electron deficiency. This spectrum is completely different from that of the calcined sample treated with plasma (Pt/CeO$_2$-c Plasma) in Fig. 1a, which evidences that the plasma treatment affects very differently the calcined and the fresh samples. Whereas, Pt at the surface of the calcined sample was reduced upon plasma treatment, Pt at the surface of the fresh
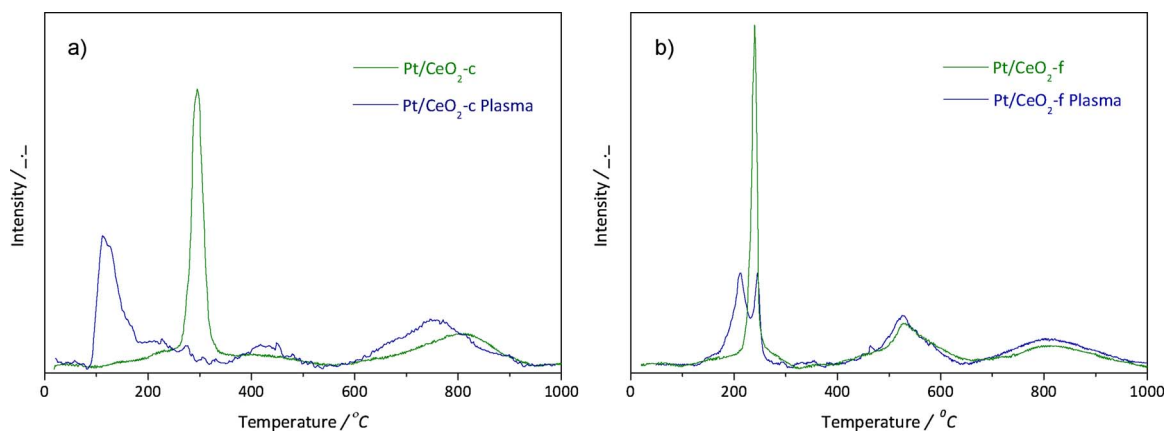
Fig. 3. TPR-H$_2$ profiles for a) calcined and calcined plasma samples and b) fresh and fresh plasma samples.
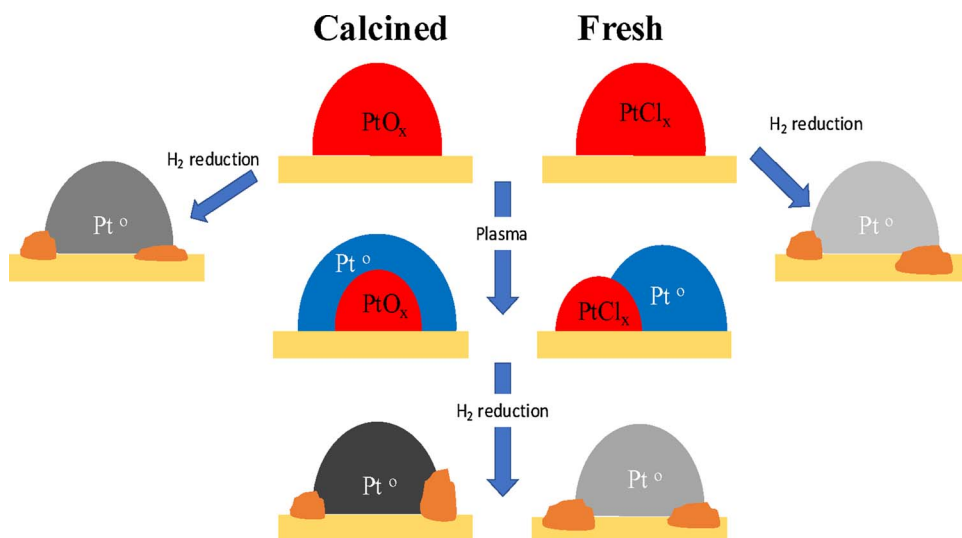

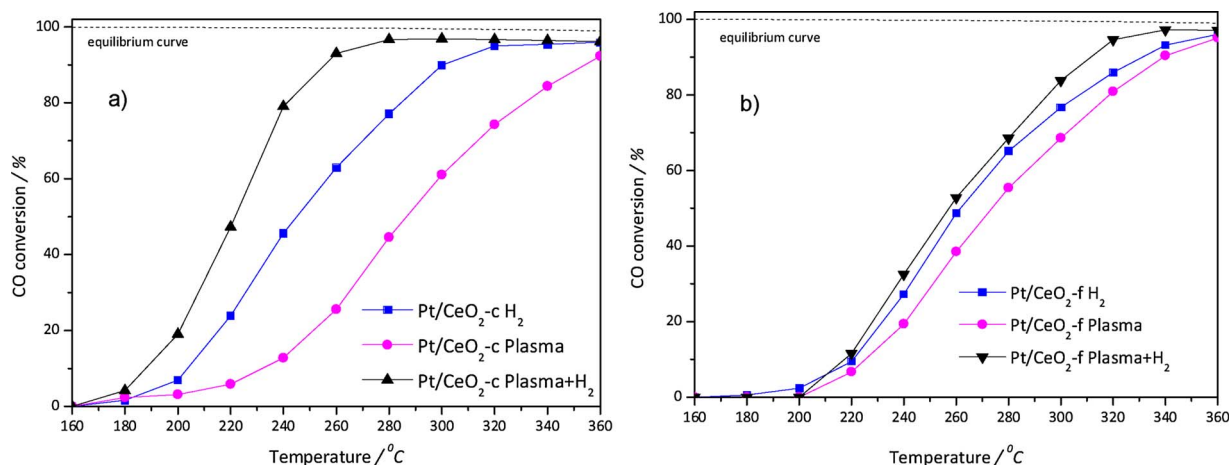**Fig. 4.** Scheme of the different type of particles formed.

Fig. 5. WGS activity of a) calcined and b) fresh samples.

sample was simultaneously reduced and oxidized, suffering something similar to a disproportionation redox process. Otherwise, the fresh sample treated with plasma and H$_2$ (Pt/CeO$_2$-f Plasma + H$_2$) only shows a single type of Pt species, with B.E. similar to those of the calcined sample (Pt/CeO$_2$-c Plasma + H$_2$).

After a deep characterization of the samples by XPS and XANES, their redox behaviour will be analysed. Temperature-programmed reduction experiments with H$_2$ (TPR-H$_2$) of the fresh and calcined

samples and those treated with plasma were carried out. TPR profiles of the fresh and calcined sample (Fig. 3) show a single peak below 400 °C, which is ascribed to the reduction of ceria in close contact with Pt. This peak shows up at lower temperature for the fresh sample than for the calcined one. This can be explained considering that during the calcination treatment some Pt-O-Ce species are formed and these species are more difficult to reduce than the (PtCl$_6$)$^{2-}$ species attached to the ceria surface in the fresh sample [15,31,32]. The reduction of ceria in close

contact with the Pt nanoparticles is carried out through a spill-over mechanism in both materials. On the other hand, samples treated with plasma, show a different behaviour. The sample calcined and treated with plasma (Pt/CeO$_2$-c-Plasma) shows a new reduction peak at around 160 °C, which is 90 °C lower than in the calcined sample not submitted to the plasma treatment (Pt/CeO$_2$-c). The generation of Pt core-shell particles (Pt^0/Pt^{n+}) with enhanced Pt-ceria interaction facilitates spill-lover and the reduction of the ceria support. Hydrogen chemisorbs better in Pt^0 than in Pt^{n+}. The Pt/CeO$_2$-c-Plasma sample has a Pt^0 shell that favours the chemisorption of H$_2$ and further reduction of the core, enhancing the reducibility of the whole system. The TPR of the Pt/CeO$_2$-f-Plasma sample shows two peaks, once centred at 180 °C and the other one centred at 240 °C. This might indicate that there are two different types of platinum species, what is in line with what we could see by XPS spectroscopy. The peak at lower temperature may be ascribed to the reduction of ceria in close proximity with reduced Pt particles upon plasma treatment. Otherwise, the peak at higher temperature, which appears at the same temperature than that observed when the catalyst was not treated with plasma, may correspond to the reduction of ceria in close proximity to the Pt species that have not been affected by plasma treatment.

It was found that plasma treatment affects in a different way to the fresh (just impregnated) or calcined catalysts. Fig. 4 recaps how the different treatments affect the catalyst and the type of particles formed. Plasma and further treatments generate Pt^0 particles with different degree of interaction with the support, which depends on the sample activation process. The Pt/CeO$_2$-c-Plasma sample is very different compared to the other samples prepared by hydrogen reduction, since the binding energy of the Pt 4f$_{7/2}$ level is 0.6 eV lower than for the other samples. It suggests that these particles are electron-enriched.

The quantitative analysis of the XPS has been also performed (Table 1). Both samples follow the same tendency. The fresh and calcined samples before any treatment show a surface atomic Pt/Ce ratio of 0.041 and 0.017, respectively. When both samples were treated with plasma, the Pt surface concentration increased. This can be ascribed to two different effects, ablation of the surface and re-dispersion of the Pt particles. When the fresh and calcined samples were reduced, the surface concentration of Pt decreased in both cases, what is due to the interaction with the support. The same occurs when the plasma-treated samples are reduced, being this effect even more pronounced. This is consequent with an enhancement of the Pt-support interaction by the combination of the plasma and the hydrogen treatments.

Fig. 5 shows the WGS catalytic activity of the studied samples under model conditions (5% CO + 30% H$_2$O). For both, fresh and calcined parent catalysts, catalytic activity follows the same trend: plasma + H$_2$ > H$_2$ > plasma. It can be observed that the plasma treatment was not enough to improve the CO conversion compared with the conversion provided by a conventional reduction treatment. It is well known that Pt by itself is not a good catalyst for this reaction. The interaction with the support is one of the key factors that make Pt/CeO$_2$ a promising catalyst for this reaction. XPS and XANES analyses indicate that plasma treatment produces a strong Pt/ceria interaction. When both treatments are combined, the catalytic activity is boosted for both catalysts, although this is produced in a more pronounced way in the calcined sample. Indeed, the calcined sample exposed to cold plasma exhibited outstanding activity, reaching full conversion much earlier than the catalyst pre-treated only in hydrogen. This exceptional behaviour must be ascribed to the high electron density of Pt particles, which are stabilized by the ceria support. Thus, CO chemisorption is enhanced compared to over conventional-synthesized Pt nanoparticles. Furthermore, the interaction between these Pt particles and the support takes place at a lower temperature (TPR). In other words, the metal-support interaction is enhanced when plasma and reduction treatments are combined. In this situation, the higher reducibility and the enhanced redox properties associated with electronics perturbations occasioned by plasma treatment, result in an increased metal-support

interaction and surface electronic enrichment, which explains the excellent catalytic activity of Pt/CeO$_2$-c Plasma + H$_2$ sample.

The best catalyst obtained in this work outperforms other Pt/CeO$_2$ materials reported in the literature for WGS under the same conditions. For example, Kalamaras et al. found that Pt/CeO$_2$ catalysts reached 24.9% CO conversion at 250 °C. This result is pretty much in line with the one found for Pt/CeO$_2$-c H$_2$ or Pt/CeO$_2$-f H$_2$. However, Pt/CeO$_2$-c-Plasma + H$_2$ catalyst reaches 90% CO conversion at the same temperature, showing the spectacular effect of the plasma treatment.

4. Conclusions

From the above results, it can be concluded that the increase in the electronic density on platinum nanoparticles toguether with the reduction of ceria surface, generated by the cold Ar plasma treatment, could help to overcome water dissociation and CO activation over the Pt/CeO$_2$ catalysts in the water-gas shift reaction. In this sense, cold plasma seems to be a promising pre-treatment for metal-supported catalysts for the WGS reaction.

Appendix A. Supplementary data

Supplementary data associated with this article can be found, in the online version, at https://doi.org/10.1016/j.apcatb.2017.11.065.

References

[1] X. Chen, X. Su, B. Liang, X. Yang, X. Ren, H. Duan, Y. Huang, T. Zhang, J. Energy Chem. 25 (2016) 1051–1057.
[2] T.P. De Castro, R.P.S. Peguin, R.C.R. Neto, L.E.P. Borges, F.B. Noronha, Top. Catal. 59 (2016) 292–302.
[3] V. Del Villar, L. Barrio, A. Helmi, M.V.S. Annaland, F. Gallucci, J.L.G. Fierro, R.M. Navarro, Catal. Today 268 (2016) 95–102.
[4] M. González-Castaño, S. Ivanova, O.H. Laguna, L.M. Martínez, T.M.A. Centeno, J.A. Odriozola, Appl. Catal. B: Environ. 200 (2017) 420–427.
[5] D.C. Grinter, J.B. Park, S. Agnoli, J. Evans, J. Hrbek, D.J. Stacchiola, S.D. Senanayake, J.A. Rodriguez, Surf. Sci. 650 (2016) 34–39.
[6] P. Lu, B. Qiao, N. Lu, D.C. Hyun, J. Wang, M.J. Kim, J. Liu, Y. Xia, Adv. Funct. Mater. 25 (2015) 4153–4162.
[7] Z. Abdelouahab-Reddam, R. El Mail, F. Coloma, A. Sepúlveda-Escribano, Catal. Today 249 (2015) 109–116.
[8] A.B. Dongil, L. Pastor-Pérez, N. Escalona, A. Sepúlveda-Escribano, Carbon 101 (2016) 296–304.
[9] L. Pastor-Pérez, A. Sepúlveda-Escribano, Appl. Catal. A: Gen. 529 (2017) 118–126.
[10] A. Haryanto, S. Fernando, N. Murali, S. Adhikari, Energy Fuels 19 (2005) 2098–2106.
[11] M. Misono, N. Nojiri, Appl. Catal. 64 (1990) 1–30.
[12] C.H. Campos, P. Osorio-Vargas, N. Flores-González, J.L.G. Fierro, P. Reyes, Catal. Lett. 146 (2016) 433–441.
[13] V.A. De La Peña O'Shea, M. Consuelo Álvarez Galván, A.E. Platero Prats, J.M. Campos-Martin, J.L.G. Fierro, Chem. Commun. 47 (2011) 7131–7133.
[14] A. Huidobro, A. Sepúlveda-Escribano, F. Rodríguez-Reinoso, J. Catal. 212 (2002) 94–103.
[15] A. Sepúlveda-Escribano, F. Coloma, F. Rodríguez-Reinoso, J. Catal. 178 (1998) 649–657.
[16] J.C. Serrano-Ruiz, G.W. Huber, M.A. Sánchez-Castillo, J.A. Dumesic, F. Rodríguez-Reinoso, A. Sepúlveda-Escribano, J. Catal. 241 (2006) 378–388.
[17] C. Liu, M. Li, J. Wang, X. Zhou, Q. Guo, J. Yan, Y. Li, Cuihua Xuebao/Chin. J. Catal. 37 (2016) 340–348.
[18] Z. Tang, Q. Li, G. Lu, Carbon 45 (2007) 41–46.
[19] R.M. Navarro, J. Arenales, F. Vaquero, I.D. González, J.L.G. Fierro, Catal. Today 210 (2013) 33–38.
[20] M.C. Sanchez-Sanchez, R.M. Navarro, I. Espartero, A.A. Ismail, S.A. Al-Sayari, J.L.G. Fierro, Top. Catal. 56 (2013) 1672–1685.
[21] M. Martinelli, G. Jacobs, U.M. Graham, W.D. Shafer, D.C. Cronauer, A.J. Kropf, C.L. Marshall, S. Khalid, C.G. Visconti, L. Lietti, B.H. Davis, Appl. Catal. A: Gen. 497

(2015) 184–197.

[22] E.O. Jardim, S. Rico-Francés, F. Coloma, J.A. Anderson, E.V. Ramos-Fernandez, J. Silvestre-Albero, A. Sepúlveda-Escribano, Appl. Catal. A: Gen. 492 (2015) 201–211.

[23] E.V. Ramos-Fernández, B. Samaranch, P. Ramírez de la Piscina, N. Homs, J.L.G. Fierro, F. Rodríguez-Reinoso, A. Sepúlveda-Escribano, Appl. Catal. A: Gen. 349 (2008) 165–169.

[24] E.V. Ramos-Fernández, A. Sepúlveda-Escribano, F. Rodríguez-Reinoso, Cat. Commun. 9 (2008) 1243–1246.

[25] S. Rico-Francés, E.O. Jardim, T.A. Wezendonk, F. Kapteijn, J. Gascon, A. Sepúlveda-Escribano, E.V. Ramos-Fernandez, Appl. Catal. B: Environ. 180 (2016) 169–178.

[26] NIST.

[27] E.V. Ramos-Fernández, J. Ruiz-Martínez, J.C. Serrano-Ruiz, J. Silvestre-Albero, A. Sepúlveda-Escribano, F. Rodríguez-Reinoso, Appl. Catal. A: Gen. 402 (2011) 50–58.

[28] R. Buitrago-Sierra, M.J. Garcia-Fernandez, M.M. Pastor-Blas, A. Sepulveda-Escribano, Green Chem. 15 (2013) 1981–1990.

[29] S.L. Swartz, J. Am. Chem. Soc. 124 (2002) 12923–12924.

[30] A. Trovarelli, Catalysis by Ceria and Related Materials, Imperial College Press, London, 2002.

[31] M. Abid, V. Paul-Boncour, R. Touroude, Appl. Catal. A: Gen. 297 (2006) 48–59.

[32] J. Rynkowski, J. Farbotko, R. Touroude, L. Hilaire, Appl. Catal. A: Gen. 203 (2000) 335–348.